Mg–MOF–74/Polyvinyl acetate (PVAc) mixed matrix membranes for CO_2 separation

Srabani Majumdar[1], Begum Tokay[1,*], Violeta Martin-Gil[2], James Campbell[1], Roberto Castro-Muñoz[2], Mohd Zamidi Ahmad[2], Vlastimil Fila[2]

[1]Chemical and Environmental Engineering Department, Advanced Materials Research Group, University of Nottingham, NG7 2RD, Nottingham, UK.

[2]Department of Inorganic Technology, University of Chemistry and Technology Prague, Technická 5, 16628 Prague 6, Czechia.

* Address correspondence to begum.tokay@nottingham.ac.uk

Keywords: Mg-MOF-74; CPO-27(Mg); mixed matrix membranes; CO_2/CH_4; activation; PVAc

Highlights:

- Mg-MOF-74 and PVAc show good compatibility at interface.
- Competitive adsorption in Mg-MOF-74/PVAc membranes increases both permeability and selectivity.
- Mg-MOF-74 activation time influences permeability and selectivity of Mg-MOF-74/PVAc membranes.
- Mg-MOF-74 incorporation in MMMs reduces the effect of plasticization.

Abstract

In this study, Mg-MOF-74 crystals were synthesised in order to prepare polymer/Mg-MOF-74 mixed matrix membranes (MMMs) for CO_2/CH_4 separation. Activation temperature and time of the Mg-MOF-74 crystals were determined in order to enhance the performance of polymer/Mg-MOF-74 mixed matrix. The Mg-MOF-74 crystals were then incorporated into polyvinyl acetate (PVAc) matrix to form dense MMMs by a solvent-casting method. After the structural characterisation of the prepared membranes, their CO_2/CH_4 separation properties were determined by measuring mixed gas permeabilities at 6 and 15 bar with a Wilke-Kallenbach method at steady-state. SEM image of MMM showed there were no visible voids at the MOF/polymer interface. The highest BET area of Mg-MOF-74 crystals was measured when activiation was performed at 150 ^oC for 24 h under vacuum. Mixed gas permeability measurements of the membranes showed that both CO_2 permeability and selectivity were improved with the increasing amount of MOF suggesting strong adsorption selectivity of Mg-MOF-74 for CO_2. Activation time of Mg-MOF-74 crystals influenced the permeability and selectivity of MMMs. Incorporation of Mg-MOF-74 helped reducing the effect of plasticization.

1. Introduction

Carbon dioxide/methane separation is important for natural gas processing because CO_2, which is a contaminant in natural gas wells, decreases the energy content of the gas, and becomes acidic and corrosive in the presence of water. Conventional CO_2 capture processes (e.g. cryogenic distillation and absorption using amines) require high levels of energy consumption [1]. Therefore an efficient, environmental friendly, economically viable capture process is needed. Membrane-based separation technologies have been prefered due to their ease of operation and energy-saving potential [2].

Polymeric membranes are the current state-of-the-art for CO_2/CH_4 separations [3]. However there is a trade-off between permeability and selectivity that limits their performance [4]. Incorporation of inorganic filler particles to produce mixed matrix membranes (MMMs) can overcome these issues. Porous filler particles, such as zeolites and carbon molecular sieves [5-10], can increase the permselectivity of membranes. However, poor interaction at the interface between inorganic and polymer phases is a major challenge to be addressed [11].

Metal–organic frameworks (MOFs), which comprised of metal ions connected by organic linkers, can be the most promising candidates for MOF-polymer MMMs due to their diversity and flexibility in structure. They possess ultra-high porosity (up to 90% free volume) and enormous internal surface areas [12, 13]. They can be synthesised with controlled pore sizes [14], surface functionalities and chemical properties [15] by changing the combination of metal and linker. Another advantage of MOFs lie in the fact that the organic linker in the structure improves their affinity to the polymer chains of membranes above that of other filler particles.

Several MOF-based MMMs have been prepared with improved performance for gas separations using both low and high flux glassy (e.g., Matrimid, Polyvinyl Acetate (PVAc) and Ultem) and high flux rubbery (e.g., Polydimethyl siloxane) polymers [16-19]. Some of these studies investigated MOFs with small pores, which can separate molecules by size exclusion. Adams et al. added CuTPA to PVAc and the MMM exhibited increased selectivity for various gas mixtures [16]. Incorporation of 15 wt% MOF particles into polymer matrix improved the CO_2/CH_4 selectivity of pure polymer up to 34%. Ordonez et al. reported 4 times higher ideal CO_2/CH_4 selectivity for ZIF-8/Matrimid MMMs with 50 wt% ZIF-8 loading [20]. However, the CO_2 permeability decreased 80% (to 4.72 Barrer) in comparison to pure Matrimid (22.31 Barrer). Polyimide MMMs containing ZIF-90/6FDA, on the other hand, showed permeability and selectivity reaching up to 3000 Barrer and 19.6 at 1 bar pressure drop, respectively [21].

MOFs with mesoporous cavities have also been investigated in order to overcome sorption and mass transfer limitations. These MOFs exhibit extremely high CO_2 adsorption capacities [22]. Perez et al. showed that with incorporation of 30 wt% MOF-5 in a Matrimid®-PI polymer, permeability of gases can be increased by 120% while ideal selectivity remained constant [23]. Zornoza et al. fabricated MMMs using amine functionalized MIL-53 in polysulfone [24]. Mixed matrix membranes containing 40 wt% MIL-53 exhibited 30 selectivity for CO_2/CH_4 separation. Shahid et al. enhanced the single gas CO_2 permeability and ideal CO_2/CH_4 selectivity two times to 24 Barrer and 66, respectively, with 30 wt% MIL-53(Al) incorporation into Matrimid® polymer [25].

Selecting the appropriate type is a challenge for successful MOF-polymer MMM preparation. In addition, activation of the MOF crystals in order to access the internal porosity and remove the trapped molecules/solvents are critical [26]. Sometimes activation can be incomplete or distructive as a result of retention of molecules or collapse of the porous structure upon removal of the supporting solvent molecules, respectively. One of the key criteria for effective CO_2/CH_4 separations is selecting a MOF with a high CO_2 adsorption capacity. M-MOF-74 particles (also known as CPO-27-Mg; where M is a metal e.g. Ni, Mg) incorporated into polymer membranes has received attention for CO_2 separations, due to their exceptional CO_2 adsorption capacities. Mg-MOF-74 in particular has displayed high adsorption capacity of 380 $mg.g^{-1}$ [27]. In addition, several studies reported the high separation selectivity of CO_2 over CH_4. Dietzel et al. showed a strong preference for CO_2 with respect to CH_4 or N_2 under dynamic conditions using Ni-MOF-74 powder [28]. Britt et al. exhibited that Mg-MOF-74 crystals adsorbs 3.9 mmol CO_2 per gram during breakthrough experiments with a 80% CH_4/20% CO_2 mixture at atmospheric pressure and room temperature [29]. Krishna reported CO_2/CH_4 seperation selectivities up to 200 via simulating CO_2/CH_4 separation in an adsorption bed [30]. High CO_2 adsorption capacity and separation selectivity suggest that Mg-MOF-74 is a good candidate for synthesizing high-performance CO_2 selective membranes.

A few studies investigated the performance of M-MOF-74 incorporated MMMs for gas separations. Bachman and Long showed that the incorporation of ~23% of Ni-MOF-74 nanocrystals into a range of polymers can improve ideal CO_2/CH_4 selectivities from 6 to 12 in comparison to neat polymers [31]. The CO_2 permeabilities are also improved significantly, where the polymer phases are 6FDA-DAM (626 to 1035 Barrer) and 6FDA-durene (518 to 715 Barrer). Only for Ni-MOF-74/Matrimid® was a slight decrease in CO_2 permeability observed from 9.55 to 9.31 Barrer with inclusion of MOF crystals. Bae and Long prepared MMMs with Mg-MOF-74 nanocrystals (in the range of 10-20 wt% particle loading) in two rubbery (PDMS and XLPEO) and one glassy (polyimide) polymer for CO_2 removal from N_2.

Ideal selectivities are improved 1.3-1.6 times for all MOF/polymer MMMs compared to neat polymers. However, the CO_2 permeability (850 Barrer) is increased only for MOF/polyimide membranes, with 10 wt% MOF inclusion [32].

In this study, we investigated the effect of activation and incorporation of Mg-MOF-74 crystals on the performance of Mg-MOF-74/PVAc MMMs. PVAc was selected as a low Tg polymer that has low gas permeabilities that do not alter the contribution of the MOF phase to overall MMM transport [33]. Moreover, PVAc is a cheap polymer with high CO_2 adsorption capability [34]. Mg-MOF-74 was chosen as it exhibits one of the highest CO_2 adsorption capacity and adsorption selectivity when compared to other MOFs including other metal forms of MOF-74 [35, 36]. The separation properties of the MMMs prepared were characterized by CO_2/CH_4 mixed gas streams.

2. Experimental

2.1. Materials

For Mg-MOF-74 (Fig 1) synthesis, magnesium acetate tetrahydrate ($Mg(CH_3COO)_2{\cdot}4H_2O$) (99%) and 2,5-dihydroxyterephthalic acid (H_4DHTP) (98%) were purchased from Sigma-Aldrich. Dimethylformamide (DMF, 99.98%), ethanol (99.99%), methanol (99.99%) and toluene (99.99%) were obtained from Fisher Scientific UK Ltd. PVAc (Fig 1) was purchased from Sigma Aldrich with an average molecular weight of 500,000 by GPC and relative density of 1.191 g cm^{-3}. All chemicals were used as received without further purification.

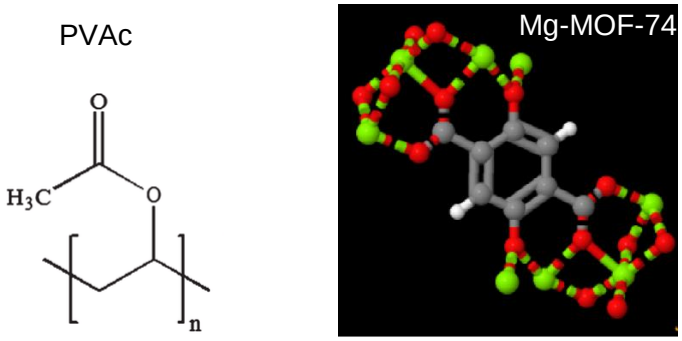

Fig. 1. Chemical structures of PVAc and Mg-MOF-74 (red: oxygen, grey: carbon, green: Mg, white: hydrogen) [37].

2.2. Synthesis of Mg-MOF-74 crystals

The Mg-MOF-74 crystals were prepared using the synthesis devised by Campbell and Tokay [38]. First, approximately 0.4 g of H_4DHTP was mixed in 10 ml DMF using a magnetic stirrer until the ligand had completely dissolved. A metal salt solution was then prepared by dissolving 1.2 g of magnesium acetate tetrahydrate in a mixture of 6 ml of DMF, 2 ml of

water and 2 ml of ethanol. The organic ligand solution was added dropwise to the metal salt solution. Once all the ligand solution added to the metal salt solution, the mixture was transferred to a 45 ml Parr reaction vessel with a Teflon® liner. The sealed vessel was placed into an oven at 125 °C for 6 h. After solvothermal synthesis, crystal samples were washed with 25 ml of DMF three times over 48 h, followed by washing with 25 ml of methanol three times over 6 days. The samples were then allowed to dry at ambient conditions before activation under vacuum at 100 and 150 ^{o}C up to 48 h.

2.3. Preparation of Mg-MOF-74 incorporated PVAc mixed matrix membranes

Membranes were prepared by solution-casting technique [39]. The MOF/PVAc membranes containing up to 20 wt% Mg-MOF-74 crystals were first dispersed in toluene, the suspension was mixed overnight on a magnetic stirrer before adding the polymer (with a 25/75 polymer/solvent wt% ratio). After the polymer addition, the mixture was stirred overnight. The film was cast on to a Teflon® surface after cleaning with ethanol. The initial thickness of the films was set to 550 µm using a casting knife. The film was placed in a fume cupboard at 25 ^{o}C overnight and then dried in a vacuum oven at 60 ^{o}C for 48 h in order to remove residual solvent. Membranes were cooled down to room temperature inside the vacuum oven and stored in a desiccator. The thickness of the dried membranes varied from 45 µm to 75 µm. Pure PVAc membranes were also prepared using a similar protocol but omitting the particle dispersion step.

2.4. Characterisation of MOF crystals and membranes

Structural and morphological characterisation of MOF particles and membranes was performed by X-ray diffraction (XRD) and scanning electron microscopy (SEM). XRD patterns were obtained by a Siemens D500 using CuKα (λ = 1.54 Å) as a radiation source. The X-ray scans were taken in the 2θ range of 4^{o} and 20^{o} (MOFs) and 5° to 50° (membranes) at a rate of 0.05° s^{-1}. To determine the morphology and crystal size, SEM analysis was carried out using JEOL 6400 scanning electron microscope. MOF particles were attached on sample holder with an adhesive carbon foil. Membrane cross-sections were obtained by cryogenic fracturing in liquid nitrogen. The samples were then coated with platinum (using a Polaron sputter coater) to avoid charging of sample surfaces. The images were used to evaluate the MOF crystals, MOF-polymer interface, the dispersion of MOF particles and the final membrane thickness. Brunauer–Emmett–Teller (BET) surface areas and CO_2 and CH_4 adsorption/desorption isotherms (at 25 ^{o}C) were determined using a Micromeritics, TriStar II 3020, Norcross, GA gas adsorption analyser. Thermal Gravimetric Analysis (TGA, TA Q500) of Mg-MOF-74 crystals, pure PVAc and and Mg-MOF-74 containing membranes were performed by heating ~20 mg of sample in an alumina crucible. The measurements were carried out under nitrogen flow (20 ml min^{-1}) between 25 and 600

°C with a heating rate of 2 and 20 °C min^{-1} for crystals and membranes, respectively. Differential scanning calorimetry (DSC, TA Q100) was carried out to determine the glass transition temperature of the membranes, thus allowing the interaction between PVAc and MOF fillers to be understood. The samples were heated under a nitrogen atmosphere (flow rate= 50 ml min^{-1}) with a heating rate of 5 °C min^{-1} from 0 °C to 100 °C. Sample weight was maintained at 10 mg. All measurements were repeated three times.

2.5. Mixed gas separation measurements

The mixed gas separation performances of the pure and mixed matrix membranes were measured via Wicke–Kallenbach technique [40], using binary mixtures of CO_2:CH_4 (50:50 and 90:10 vol%) with He as a sweep gas. The measurements were conducted at 25 °C with a feed pressure of 6 bar. For plasticization effect, feed pressure was set to 15 bar. We also investigated the influence of temperature separation peformace at 35 °C, near T_g. The gas flowrates were controlled by Bronkhorst mass flow controllers at CO_2= 20 ml.min^{-1}, CH_4= 20 ml.min^{-1} and He= 5 ml.min^{-1}. The steady state permeate and retentate gas mixture compositions were measured using a Thermo Electron Focus Gas Chromatograph (Czechia) equipped with a methanizer and flame ionisation detector and an Agilent 7890 GC/MS system (Nottingham).

The permeability, P_i (cm^3.cm.$cmHg^{-1}$.s-1.cm^{-2}) of permeating species, i was defined by the following equation [35] [41]

$$P_i = \frac{{y_i}^P.F^s.l}{A({y_i}^R.P^R - {y_i}^P.P^P)} \quad (1)$$

Where F^s, is the flow rate of sweep gas ($cm^3.s^{-1}$), l ,the thickness of the membrane (cm), A, is the membrane area (cm^2), ${y_i}^R, and\ {y_i}^P$ are the mole fraction of i, in the retentate and permeate stream respectively, P^R (cmHg) and P^P (cmHg) are the pressure in retentate and permeate respectively. It is also convenient to express permeability in Barrer (1 Barrer = 10^{-10} cm^3 (STP) cm s^{-1} cm^{-2} $cmHg^{-1}$).

The separation factor was calculated using Equation 2,

$$\alpha_{CO_2/CH_4} = \frac{y_{CO_2}\ /\ y_{CH_4}}{x_{CO_2}\ /\ x_{CH_4}} \quad (2)$$

Where y_{CO_2} and y_{CH_4} are the mole fractions of the CO_2 and CH_4 in the permeate stream respectively, x_{CO_2} and x_{CH_4} are their corresponding mole fractions in the feed stream.

3. Results and Discussions

3.1. Characterisation of Mg-MOF-74

The XRD pattern of activated (at 150 °C for 24 h under vacuum) and SEM image of as-synthesised Mg-MOF-74 crystals was shown in Fig 2. The crystalline structure of samples

were confirmed by the most prominent characteristic peaks of Mg-MOF-74 peaks, indicated by dashed lines in Fig 2a (6.7°, 11.7° and 18°) [32]. The SEM image of the as-synthesised MOF-74 particles in Fig 2b shows regular structure of Mg-MOF-74, with particle size ranging from 1 to 5 µm. Some of the larger particles are agglomerates of smaller crystals.

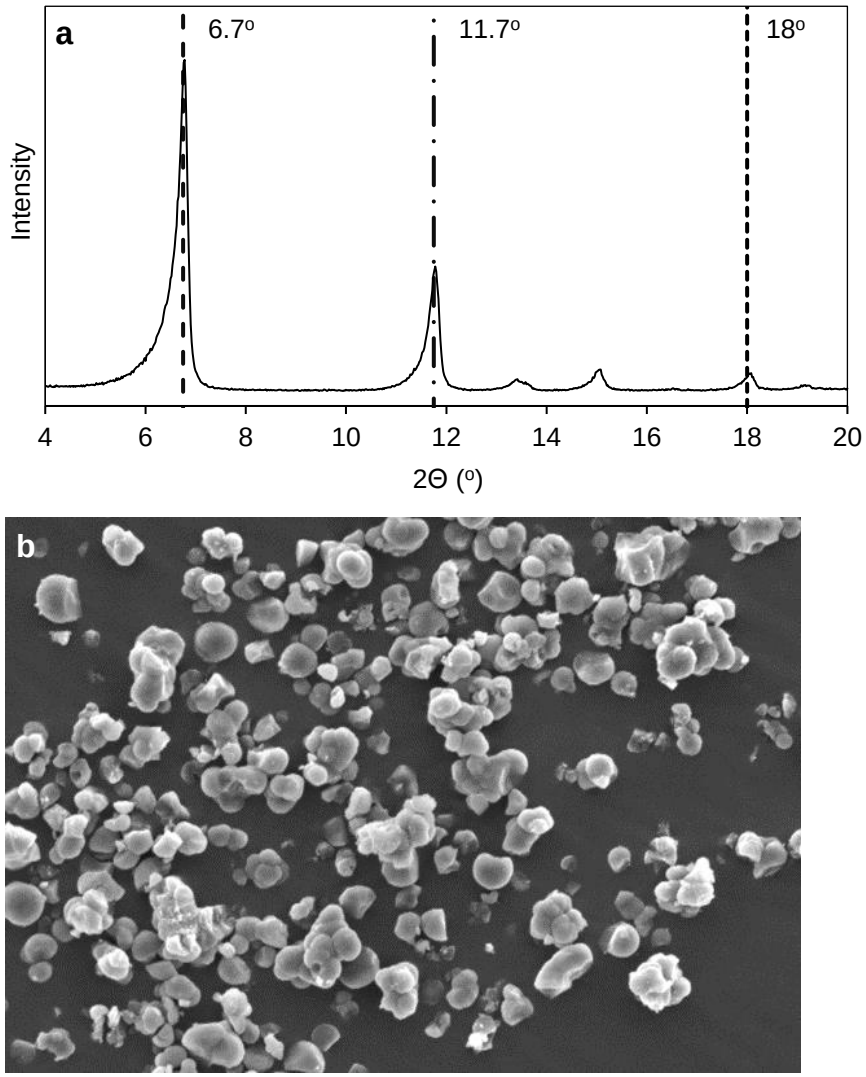

Fig. 2. (a) The XRD pattern of activated (at 150 ºC for 24 h under vacuum) and (b) SEM image of as-synhesised Mg-MOF-74 crystals.

Table 1 summarizes the BET areas of Mg-MOF-74 crystals activated at various temperatures and durations. Activation at 100 ºC under vacuum resulted with the BET areas of around 250 and 283 m^2 g^{-1} for 24 and 36 h, respectively. This suggests 100 ºC is not adequate to clear the pores from solvent residue. Increasing the activation temperature to 150 ºC for 16 h was increased the BET area up to 325 ± 2.7. The data showed that the highest BET area (402 m^2 g^{-1}) was measured for 24 h after increasing the activation temperature to 150 ºC. This may be attributed to removing more solvent residues and thus increasing pore accesibility. However, after activation at 150 ºC for 36 h under vacuum, the

BET area was reduced. This may be an indication of degradation. Interestingly, for 48 h activation, there was no porosity and thus no BET area was estimated. This may be due to the long activation times, especially under vacuum, at 150 ^{o}C that degrades the MOF stucture. Mg-MOF-74 is expected to be stable between ca. 350-400 ^{o}C, shown *via* TGA result [42]. However, solvent, which is used during the synthesis may have an influence on the stability of Mg- MOF-74 crystals under vacuum at high temperatures. In literature, various activation conditions was reported for Mg-MOF-74 crystals such as 200 ^{o}C for 6 h under vacuum when only DMF was used as solvent [29]. In contrast, Pu et al activated Mg-MOF-74 crystals at 120 ^{o}C for 2 h that were synthesised using DMF/water/ethanol mixture as solvent [43]. In another study, crystals were activated at 200 ^{o}C for 4 h under vacuum [44]. We did not investigate this further whilst we fixed the activation conditions as 150 ^{o}C for 24 h for Mg-MOF-74 crystals.

Table 1. BET areas of Mg-MOF-74 crystals activated at 100 and 150 ^{o}C for 16-48 h under vacuum (Degassing at 150 ^{o}C, 12 h).

Temperature (^{o}C)	Time (h)	BET area (m^2 g^{-1})
100	24	250 ± 5.3
	36	283 ± 6.7
150	16	325 ± 2.7
	24	402 ± 3.8
	36	355 ± 7.2
	48	N/A

Adsorption and desorption isotherms of CO_2 and CH_4 on the Mg-MOF-74 crystals at 298 were plotted in Fig 3. The steep slope in the low-pressure region of the CO_2 isotherm indicates a strong adsorption of CO_2 onto Mg-MOF-74. On the other hand, the CH_4 isotherm was linear, which demonstrates a weak interaction between CH_4 and MOF crystals, agreeing with the reports in literature [28, 29, 42, 45, 46]. The CO_2 uptake at 25 ^{o}C, 1 bar is approx. 20.6 cm^3 g^{-1} while the CH_4 uptake is only 2 cm^3 g^{-1}. Adsorption and desorption branches shown in these plots overlap with each other, without hysteresis. These suggest that the adsorption process is reversible and fast adsorption and desorption kinetics are probably expected.

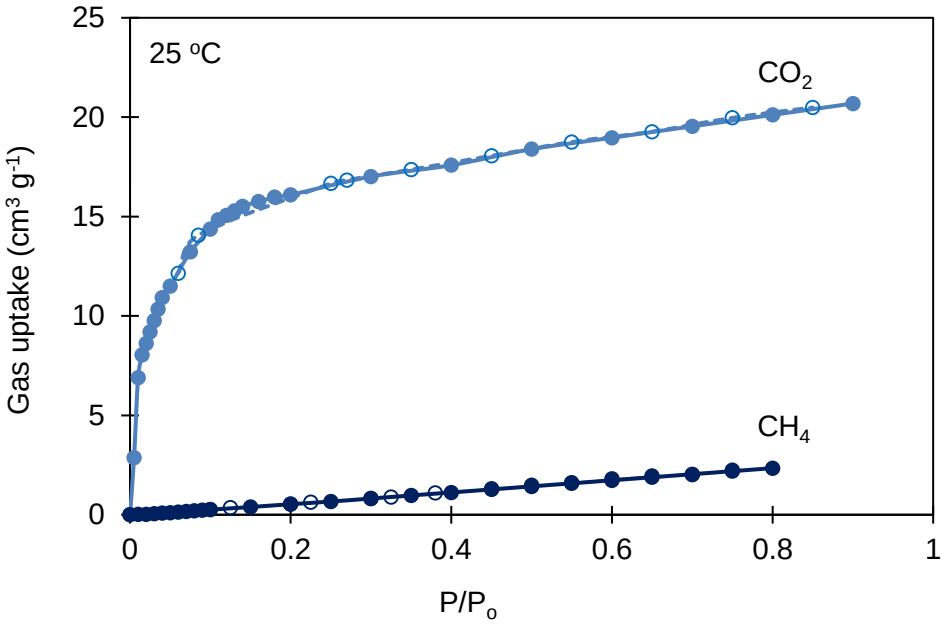

Fig. 3. Adsorption and desorption isotherms of CO_2 and CH_4 on Mg-MOF-74; open symbols, adsorption; filled symbols, desorption.

In Fig. 4, the TGA diagram of activated (150 °C, 24 h) sample was presented. There is a slight weight loss (5%) until 150 °C that is attributed to the trapped DMF (boiling point 153 °C), water and methanol in the pores. There was a slight weight loss (~5%) between ca. 150 and 350 °C for Mg-MOF-74 crystals, most probably resulted from the loss of crystal water [43]. This may be the reason for loss of porosity and thus the BET areas observed for crystals, which are activated at 150 °C for 48 h, under vacuum. At temperatures above 350 °C, the decomposition of the framework started, showing a more dramatic weight loss, which was in good agreement with those reported in literature [42, 43].

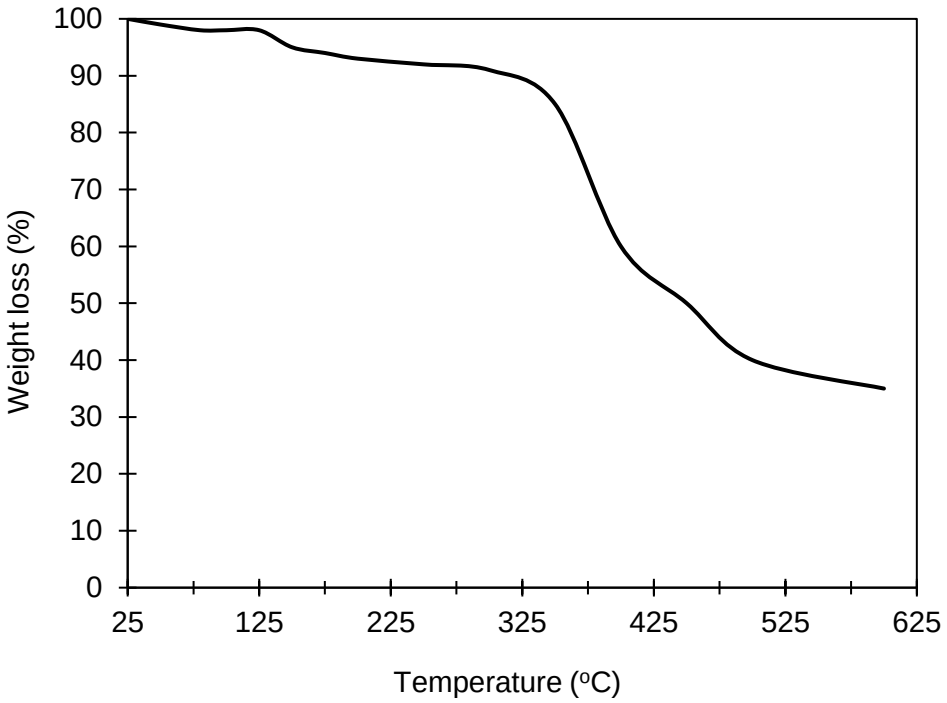

Fig. 4. TGA curve for activated (150 °C, 24 h under vacuum) Mg-MOF-74 crystals.

3.2 Membrane characterization

3.2.1. Structural properties

Fig 5 shows the XRD patterns of MMMs in comparison to Pure PVAc and Mg-MOF-74 crystals. The comparison shows that Mg-MOF-74 particles retained their crystallinity (peaks at 6.8° and 11. 7°) as there was no considerable loss in crystallinity. This suggests that MOF particles conserved their crystallinity after all mechanical and thermal treaments through MMM preparation. In the meantime, the intensity of broad PVAc peaks between 15° and 23° was reduced, which may indicate the disruption of the primary crystalline pattern in the PVAc by the incorporation of MOF particles [47]. Alternatively, the –OH group on the surface of Mg-MOF-74 and –H groups of the PVAc may link to form hydrogen bonding [1].

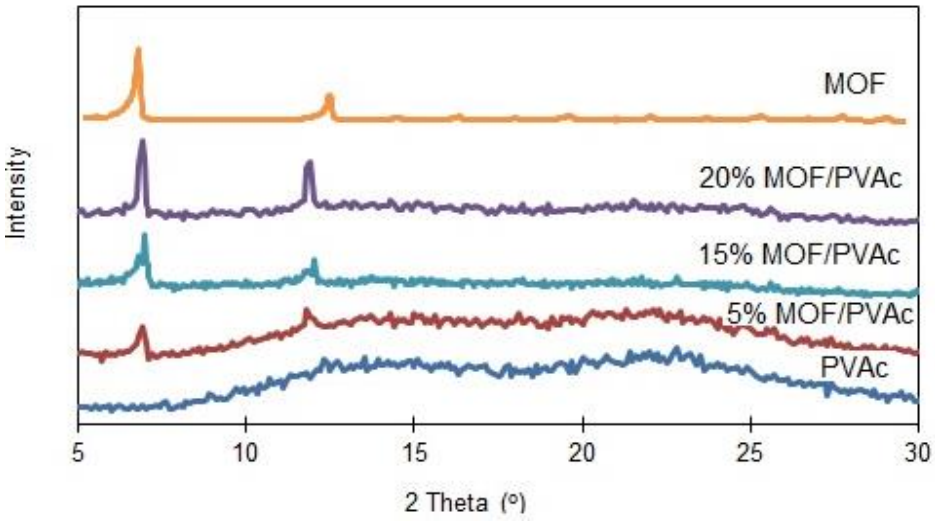

Fig. 5. The XRD patterns of Mg-MOF-74 crystals, pure PVAc membrane and the MMMs loaded with 5, 10 and 15 wt% of Mg-MOF-74 crystals (activation: 150 ºC for 24 h under vacuum).

The cross section SEM image of the MMM containing 20 wt% of Mg-MOF-74 crystals. showed generally good interface contact between MOF particles and polymer phase since no significant voids were observed at the particle/polymer interface, as similar in previous reports (Fig S1, see *Supporting Information, SI*) [16, 39]. The SEM image also showed that there was a uniform distribution of Mg-MOF-74 particles in the polymer matrix. In addition, particle agglomeration was observed The uniformity suggests that the mixing protocol applied in the membrane preparation was sufficient for good dispersion of crystals whilst they were agglomerated.

Fig. 6 exhibits the TGA curves of pure PVAc membranes and the MMMs loaded with 5, 15 and 20 wt% of Mg-MOF-74 particles. For the pure PVAc membranes, there is no considerable weight loss up to approx. 325 °C. However, the amount of residual solvent removed (until 200 ºC) was higher in mixed matrix membranes compared to the pure PVAc membrane. This difference may be attributed to the entrapped solvent molecules in the Mg-MOF-74 cavities. The weight losses between 200 ºC and 320 ºC were relatively higher in MMMs than pure PVAc membrane, as the organic structure of Mg-MOF-74 was lost at nearly 320 ºC. The weight loss at the temperature interval 200-320 ºC was 34% for the MMM containing 20 wt% Mg-MOF-74, while it was 24% and 8% for the MMM containing 15 wt% and 5 wt% Mg-MOF-74, respectively. Hence, the weight loss almost fourfold in MMMs between 200 ºC and 320 ºC when the Mg-MOF-74 loading amount fourfold, due to the loss of organic linkers in Mg-MOF-74 framework at this temperature interval.

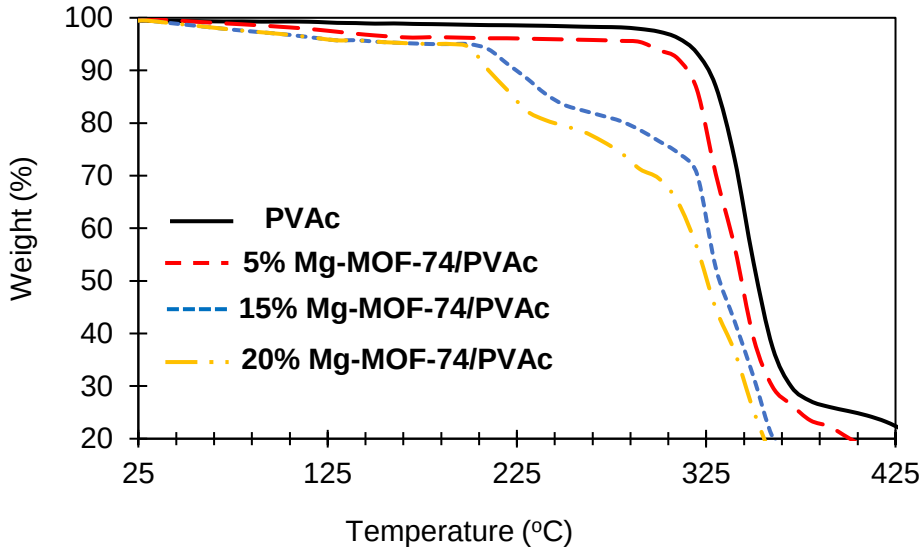

Fig. 6. TGA curves for pure PVAc membrane and the MMMs loaded with 5, 15 nd 20wt% of Mg-MOF-75 particles.

According to DSC measurements, pure PVAc showed a glass transition temperature (T_g) at about 30 °C ± 0.6. T_g values were increased by 2 to 8 °C with the incorporation of 5 to 20 wt% Mg-MOF-74 particles into PVAc matrix, respectively. This increase may suggest that the incorporation of MOFs reduces the chain flexibility of polymer [15]. Hydrogen bonding between –OH groups on the Mg-MOF-74 and the alkyl groups of polymer matrix may also be considered the increase in T_g [9, 48-50].

3.2.2. Gas separation properties

Table 2 summarizes the average mixed gas permeabilities and CO_2/CH_4 selectivities for the MMMs and the pure polymer membrane in order to compare their performances. The incorporation of the Mg-MOF-74 into the PVAc matrix successfully increased permeabilities with no considerable loss of selectivity. The increase in the permeability of CO_2 was x1.21 with 5 wt% Mg-MOF-74 loading while it was x2.42 for 15 wt% loading and x3.4 for 20 wt% loading. The permeability improvement was the result of paths inside the polymer phase generated by the Mg-MOF-74 crystals that gas molecules could pass through.

Table 2. Mixed gas CO_2/CH_4 separation performance of pure PVAc and MMMs containing 5, 15 and 20 wt% Mg-MOF-74 (activation: 150 °C for 16 h under vacuum).

Membrane	CO_2 permeability (Barrer)	CH_4 permeability (Barrer)	CO_2/CH_4 selectivity
Pure PVAc	0.71 ± 0.1	0.07 ± 0.03	10.6 ± 0.03
5 wt% Mg-MOF-74/PVAc	0.86 ± 0.1	0.07 ± 0.01	12 ± 0.1
15 wt% Mg-MOF-74/PVAc	1.72 ± 0.03	0.11 ± 0.02	15.6 ± 0.1

20 wt% Mg-MOF-74/PVAc	2.42 ± 0.1	0.11 ± 0.1	21.2 ± 0.2

Mixed gas selectivities improved in MMMs compared to the pure PVAc membrane. They gradually increased with the amount of Mg-MOF-74 particles. The selectivity was increased from 10.6 (for neat polymer) to 21.2 for 20 wt% loading. These results for MMMs suggest that the membrane has no significant interfacial defects, also validated by the SEM image. In addition to this, these results show a competitive adsorption mechanism existed between CO_2 and CH_4 as both gases can readily pass through Mg-MOF-74 pores. This indicates that the adsorption selectivity in MOF-74 favoring CO_2 over CH_4.

We studied the effect of MOF activation time on CO_2/CH_4 separation performance of MMMs containing 20 wt% Mg-MOF-74 crystals (Table 3). The data show that the CO_2 permeability and selectivity increased from 2.42 to 4.7 Barrer and 21.2 to 24.8, respectively, when MOF crystals were activated for 24 h rather than 16 h. This observation agrees well with the BET areas of MOF crystals shown in Table 1. As pore area in Mg-MOF-74 particles increases with longer activation time, the membrane could be said to have many more paths for gas passage. Therefore, it's reasonable to have enhancement on the permeability and selectivity. Further increase of MOF activation time from 24 to 36 h reduced both the CO_2 permeability and selectivity. This result may suggest that some MOF pores are collapsed more than 24 h activation, shown by BET areas of crystals and thus the CO_2 permeability and actual selectivity reduced. We expected that the reduction in the BET area also hinders the CH_4 permeability. However, there was a slight increase in the permeability that might be the result of the size of the pores that collapsed favouring more CH_4 permeation.

Table 3. Mixed gas CO_2/CH_4 separation performance of MMMs containing 20 wt% Mg-MOF-74 as a function of MOF activation time (at 150 ^oC under vacuum).

MOF activation (h)	CO_2 permeability (Barrer)	CH_4 permeability (Barrer)	CO_2/CH_4 selectivity
16	2.42 ± 0.11	0.11 ± 0.1	21.2 ± 0.2
24	4.7 ± 0.1	0.19 ± 0.02	24.8 ± 0.2
36	3.98 ± 0.13	0.22 ± 0.04	18.1 ± 0.1

Table 4 summarizes the mixed gas permeation properties of pure PVAc membranes and 20 wt% Mg-MOF-74 (activated at 150 ^oC for 24 h) incorporated MMMs at feed pressures of 6 and 15 bar. The effect of plasticization on pure PVAc is clearly evident by approx. 3 times increase in the CO_2 permeability along with 33% reduction in actual selectivity. Under the high pressure feed, the CO_2 permeability and selectivity of the MMMs reduced, in line with previously reported literature [51]. At both pressures the MMMs show higher selectivity than pure PVAc. Almost constant selectivity in favour of CO_2 with

increasing pressure is due to the high adsorption selectivity even at high pressures that favors CO_2 over CH_4 [52]. Yazaydin et al explained that the higher density of open metal sites in Mg-MOF-74 allows enhanced CO_2 adsorption than other MOFs containing open metal sites [53]. High CO_2 sorption in pure PVAc increases the chain mobility and thus the plasticization occurs. However, the incorporation of MOFs improves selectivity of MMMs at both pressures investigated, compared to pure PVAc matrix.

Table 4. Mixed gas permeation properties of pure PVAc membranes and the MMMs loaded with 20 wt% of Mg-MOF-74 particles at feed pressures of 6 and 15 bar (activation: 150 °C for 24 h under vacuum).

Mg-MOF-74 wt% in PVAc	Feed Pressure (Bar)	CO_2 permeability (Barrer)	CH_4 permeability (Barrer)	CO_2/CH_4 selectivity
0	6	0.71 ± 0.1	0.07 ± 0.03	10.6 ± 0.03
	15	2.11 ± 0.2	0.4 ± 0.1	7.2 ± 0.11
20	6	4.7 ± 0.1	0.2 ± 0.04	24.8 ± 0.2
	15	4.01 ± 0.1	0.4 ± 0.02	22.6 ± 0.3

These results also suggest that low performance and low cost polymers such as PVAc, may have be used in real gas separation applications after MOF corporation. The enhancement obtained by Mg-MOF-74 incorporation may be much more significant for blending PVAc with other polymers showing high permeability [54].

The permeabilities and CO_2/CH_4 selectivities for the low and high CO_2:CH_4 feed ratio are reported in Table 5. CO_2 permealities and CO_2/CH_4 selectivities reduced around 70% and 85% respectively, when CO_2 ratio in the feed was reduced from 50 to 10. This indicates the strong CO_2 adsorption affinity of Mg-MOF-74 crystals.

Table 5. Mixed gas permeation properties of pure PVAc membranes and the MMMs loaded with 20 wt% of Mg-MOF-74 particles for two CO_2:CH_4 ratios at feed pressure of 6 bar (activation: 150 °C 24 h under vacuum).

Mg-MOF-74 wt% in PVAc	CO_2:CH_4 ratio	CO_2 permeability (Barrer)	CH_4 permeability (Barrer)	CO_2/CH_4 selectivity
0	50:50	0.71 ± 0.1	0.07 ± 0.03	10.6 ± 0.03
	10:90	0.3 ± 0.02	0.09 ± 0.003	3.3 ± 0.1
20	50:50	4.7 ± 0.1	0.2 ± 0.04	24.8 ± 0.2
	10:90	1.92 ± 0.1	0.4 ± 0.03	4.8 ± 0.1

The effect of increasing the temperature to 35 °C (near T_g) on the permeabilities and selectivities of pure PVAc membranes and MMM loaded with 20 wt% of Mg-MOF-74

particles were investigated at 6 bar (Table S1, *see* SI). The results showed that both the CO_2 and CH_4 permeabilities were increased, whereas the CO_2/CH_4 selectivities decreased. This can be expected since permeability increases and selectivity decreases with increasing temperature for the glassy polymers. In addition, changes in diffusion coefficients generally dominate the temperature dependence of the overall permeability [55]. On the other hand, for CO_2, reductions in solubility with increasing temperature are more significant than for CH_4. Changes in the diffusion coefficient with increasing temperature cause larger increases in diffusion coefficient for the larger penetrant in a given pair and thus overall selectivity generally drops with increasing temperature. Moreover, this temperature is almost the same as the T_g of this MMMs and thus rigid polymer chains become more flexible. Therefore, the stability of MMMs was reduced and repeatability of the results were effected (Table S1).

The CO_2/CH_4 separation performance data of membranes containing approximately 5-20 wt% MOF are summarised on 2018 [56] and 2019 [57] upper bounds for mixed and single gases, respectively (Fig 7), which shows that the incorporation of Mg-MOF-74 crystals improved the separation performance of the MMMs [19, 21, 31, 58, 59].

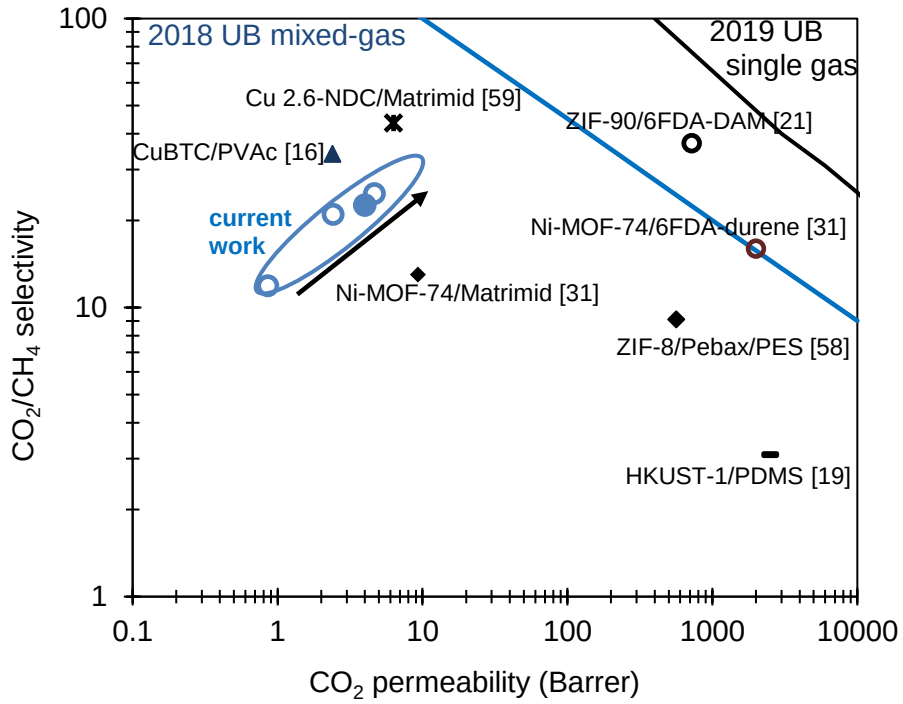

Fig. 7. CO_2/CH_4 separation performance of pure PVAc membrane and and Mg-MOF-74 incorporated MMMs, shown on the 2018 and 2019 upper bounds for mixed [56] and single [57] gas, respectively, in comparison with literature data (Black arrow shows increasing MOF content in PVAc matrix; filled circle 20 wt% Mg-MOF-74/PVAc MMM at 15 bar).

This can be attributed to the high CO_2/CH_4 sorption selectivity of Mg-MOF-74 crystals, as shown by CO_2 and CH_4 adsorption isotherms in this study and in literature [28-30].

Moreover, MOF activation time significantly enhanced both CO_2 permeability and actual selectivities of MMMs. Although MMMs performance not only depends on the MOF type and loading, MOF particle size and geometry but also on the separation porperties of polymer chosed as the continuous phase and the feed pressure, the literature data for MOF-based MMMs prepared using polymers other than PVAc and/or feed pressures higher/lower than 6 and 15 bar have also included for comparison [60]. Although CuBTC/PVAc membranes show higher permeability than Mg-MOF-74/PVAc membranes, Mg-MOF-74 crystals are more stable especially in moisture. Furthermore, Mg-MOF-74/PVAc membranes show higher selectivity than Ni-MOF-74/CE and Ni-MOF-74/Matrimid membranes with comparable permeability [31]. This is significant since the performance of Mg-MOF-74/polymer MMMs in this study may be limited by the relatively low permeability of PVAc. Therefore, Mg-MOF-74 can still be a promising additive in MMMs for CO_2/CH_4 separation compared to ZIF-8, ZIF-90, HKUST-1, Cu2.6 NDC and Ni-MOF-74, if incorporated in polyimides such as 6FDA-durene, 6FDA-DAM, PDMS, PEBAX and Matrimid® [19, 21, 31, 59] or polymer blends. Moreover, nano-sized and amine-functionalised Mg-MOF-74 crystals can provide better gas separation performance.

4. Conclusions

We successfully prepared Mg-MOF-74/PVAc MMMs for CO_2/CH_4 separation. The activation time and temperature for MOF crystals were determined as 150 ^oC and 24 h, under vacuum, respectively. The mixed gas permeability measurements showed that incorporation of Mg-MOF-74 particles into the PVAc matrix enhanced the CO_2 permeability. The results also indicated that there were competitive adsorption favoring CO_2 over CH_4 as the selectivities increased with increasing loading of Mg-MOF-74 particles. The increase in temperature near T_g reduced the stability of MMMs. Our results indicated that a low performance and low cost polymer such as PVAc, may be used in gas separation applications with increased MOF loadings. The enhancement obtained by Mg-MOF-74 incorporation may be much more significant for blending PVAc with other polymers showing high permeability.

Acknowledgement

S. Majumdar acknowledges the Erasmus Mundus scholarship and continuous support from Dr. Tokay and Dr. Fila. Dr Tokay and Dr Campbell is kindly thanked for financial support by Faculty of Engineering, University of Nottingham. Part of this work was supported by the Operational Program Prague – Competitiveness (CZ.2.16/3.1.00/24501) and “National Program of Sustainability” (NPU I LO1613) (MSMT-43760/2015). Dr Tokay thanks the Nanoscale and Microscale Centre (nmRC) for providing access to instrumentation.

References

[1] A. Brunetti, F. Scura, G. Barbieri, and E. Drioli, Membrane technologies for CO_2 separation, J Membr Sci, 359, 2010, 115.
[2] Y. Zhang, J. Sunarso, S. Liu, and R. Wang, Current status and development of membranes for CO_2/CH_4 separation: A review Int. J. Greenhouse Gas Control, 12, 2013, 84.
[3] E. Esposito, L. Dellamuzia, U. Moretti, A. Fuoco, I. Lidietta, G. logoa, and J.C. Jansen, Simultaneous production of biomethane and food grade CO_2 from biogas: an industrial case study, Energy Environ. Sci., 12, 2019,
[4] S. Kulprathipanja, R. W. Neuzil, and N.N. Li, *Separation of Fluids by Means of Mixed Matrix Membranes*, U.S. Patent 4, 219, Editor. 1988.
[5] T. W. Pechar, S. Kim, B. Vaughan, E. Marand, M. Tsapatsis, H.K. Jeong, and C.J. Cornelius, Fabrication and characterization of polyimide-zeolite L mixed matrix membranes for gas separations, J Membr Sci, 277, 2006, 195.
[6] T. W. Pechar, S. Kim, B. Vaughan, E. Marand, V. Baranauskas, J. Riffle, H.K. Jeong, and M. Tsapatsis, Preparation and characterization of a poly(imide siloxane) and zeolite L mixed matrix membrane, J Membr Sci, 277, 2006, 210.
[7] Y. Li, T. S. Chung, Z. Huang, and S. Kulprathipanja, Dual-layer polyethersulfone (PES)/BTDA-TDI/MDI co-polyimide (P84) hollow fiber membranes with a submicron PES-zeolite beta mixed matrix dense-selective layer for gas separation, J Membr Sci, 277, 2006, 28.
[8] M. Anson, J. Marchese, E. Garis, N. Ochoa, and C. Pagliero, ABS copolymer-activated carbon mixed matrix membranes for CO_2/CH_4 separation, J Membr Sci, 243, 2004, 19.
[9] D.Q. Vu, W.J. Koros, and S.J. Miller, Mixed matrix membranes using carbon molecular sieves. II, J Membr Sci, 211, 2003, 335.
[10] C.Y. Chuah, K. Goh, Y. Yang, H. Gong, W. Li, H.E. Karahan, M.D. Guiver, R. Wang, and T.-H. Bae, Harnessing Filler Materials for Enhancing Biogas Separation Membranes, Chemical Reviews, 118, 2018, 8655.
[11] D. Sen, H. Kalipcilar, and L. Yilmaz, Development of zeolite filled polycarbonate mixed matrix gas separation membranes, Desalination, 200, 2006, 222.
[12] M. Eddaoudi, J. Kim, N. Rosi, D. Vodak, J. Wachter, M. O'Keeffe, and O.M. Yaghi, Systematic design of pore size and functionality in isoreticular MOFs and their application in methane storage, Science, 295, 2002, 469.
[13] R. F. Bruinsma, P. G. D. Gennes, J. B. Freund, and D. Levine, Letter To Nature, Nature, 427, 2004, 523.
[14] R. Matsuda, R. Kitaura, S. Kitagawa, Y. Kubota, R. V Belosludov, T. C. Kobayashi, H. Sakamoto, T. Chiba, M. Takata, Y. Kawazoe, and Y. Mita, Highly controlled acetylene accommodation in a metal-organic microporous material, Nature, 436, 2005, 238.
[15] S. Kitagawa, S. Noro, and T. Nakamura, Pore surface engineering of microporous coordination polymers, Chem Commun, 7, 2006, 701.
[16] R. Adams, C. Carson, J. Ward, R. Tannenbaum, and W.J. Koros, Metal organic framework mixed matrix membranes for gas separations, Micropor. Mesopor. Mater., 131, 2010, 13.
[17] F. Zhang, et al., Hydrogen Selective NH_2-MIL-53(Al) MOF Membranes with High Permeability, Adv. Funct. Mater., 22, 2012, 3583.
[18] Y. Zhang, I.H. Musseman, J.P. Ferraris, and K.J. Balkus, Jr., Gas permeability properties of Matrimid® membranes containing the metal-organic framework Cu-BPY-HFS, Journal of Membrane Science, 313, 2008, 170.
[19] A. Car, C. Stropnik, and K.V. Peinemann, Hybrid membrane materials with different metal–organic frameworks (MOFs) for gas separation, Desalination, 200, 2006, 424.
[20] M.J.C. Ordoñez, K.C. Balkus Jr, J.P. Ferraris, and I.H. Musselman, Molecular sieving realized with ZIF-8/Matrimid® mixed-matrix membranes, J Membr Sci, 361, 2010, 28.
[21] T.H. Bae, J.K. Lee, W. Qiu, W.J. Koros, C.W. Jones, and S. Nair, A high-performance gas -separation membrane containing submicrometer-sized metal-organic framework crystals, Angew. Chem. Inter. Ed. , 49, 2010, 9863.

[22] E. Barea, F. Turra, and J.A. Rodriguez-Navarro, *Separation and purification of gases by MOFs* in *Metal organic frameworks: Applications from catalysis to gas storage*, D. Farrusseng, Editor. 2011, Wiley.
[23] E.V. Perez, J. Balkus, K.V.,, J.P. Ferraris, and I.H. Musselman, Mixed-matrix membranes containing MOF-5 for gas separations, J Membr Sci, 328, 2009, 165.
[24] B. Zornoza, A. Martinez-Joaristi, P. Serra-Crespo, C. Tellez, J. Coronas, J. Gascon, and F. Kapteijn, Functionalized flexible MOFs as fillers in mixed matrix membranes for highly selective separation of CO_2 from CH_4 at elevated pressures, Chem Comm, 47, 2011, 9522.
[25] S. Shahid and K. Nijmeijer, High pressure gas separation performance of mixed-matrix polymer membranes containing mesoporous Fe(BTC) J Membr Sci, 459, 2014, 33.
[26] O. K. Farha and J.T. Hupp, Rational Design, Synthesis, Purification, and Activation of Metal−Organic Framework Materials, Acc. Chem. Res., 43, 2010, 1166.
[27] A.O.Yazaydin, R.Q.Snurr, T.H.Park, K. Koh, J. Liu, M. D. Levan, A. I. Benin, P. Jakubczak, M. Lanuza, D. B. Galloway, J. J. Low, and R.R. Willis, Screening of metal-organic frameworks for carbon dioxide capture from flue gas using a combined experimental and modelling approach, J Am Chem Soc, 131, 2009, 18198.
[28] P.D.C. Dietzel, V. Besikiotis, and R. Blom, Application of metal–organic frameworks with coordinatively unsaturated metal sites in storage and separation of methane and carbon dioxide, Journal of Materials Chemistry, 19, 2009, 7362.
[29] D. Britt, H. Furukawa, B. Wang, T. G. Glover, and O.M. Yaghi, Highly efficient separation of carbon dioxide by a metal-organic framework replete with open metal sites, PNAS, 106, 2009, 20637.
[30] R. Krishna, Methodologies for evaluation of metal–organic frameworks in separation applications, RSC Advances, 5, 2015, 52269.
[31] J.E. Bachman and J.R. Long, Plasticization-resistant Ni_2(dobdc)/polyimide composite membranes for the removal of CO_2 from natural gas, Enviro Sci Commun, 9, 2016, 2031.
[32] T.-H. Bae and J.R. Long, CO_2/N_2 separations with mixed-matrix membranes containing Mg_2(dobdc) nanocrystals, Energy Environ Sci, 6, 2013, 3565.
[33] R.T. Adams, J.S. Lee, T.-H. Bae, J.K. Ward, J.R. Johnson, C.W. Jones, S. Nair, and W.J. Koros, CO_2-CH_4 permeation in high zeolite 4A loading mixed matrix membranes, J Membr Sci, 367, 2011, 197.
[34] Z. Shen, McHugh M.A., Xu J., J. Belardi, S. Kilic, A. Mesiano, Bane A., C. Karnikas, E. Beckman, and R. Enick, CO2-solubility of oligomers and polymers that contain the carbonyl group, Polymer, 44, 2003, 1491.
[35] S.R. Caskey, A.G.W. Foy, and A.J. Matzger, Dramatic tuning of carbon di oxide uptake via metal substitution in a coordination polymer with cylindrical pores, J Am Chem Soc, 130, 2008, 10870.
[36] R. Bétard, A. Zander, and D. Fischer, A Dense and homogeneous coatings of CPO27-Mg type metal–organic frameworks on alumina substrates, Cryst Eng Comm, 12, 2010, 3768
[37] C. R. Groom, I. J. Bruno, M. P. Lightfoo, and S.C. Ward, CDC Database, Acta Cryst, B72, 2016, 171.
[38] J. Campbell and B. Tokay, Controlling the size and shape of Mg-MOF-74 crystals to optimise film synthesis on alumina substrates, Micropor Mesopor Mater, 251, 2017, 190.
[39] C. Atalay-Oral, B. Tokay, A. Erdem-Senatalar, and T.-E. S.B., Ferrierite-poly(vinyl acetate) mixed matrix membranes for gas separation: A comparative study, Micropor Mesopor Mater, 259, 2018, 17.
[40] K. Soukup, P. Schneider, and O. Šolcová, Comparison of Wicke-Kallenbach and Graham's diffusion cells for obtaining transport characteristics of porous solids, Chem Eng Sci, 63, 2008, 1003.
[41] M.L. Cecopieri-Gomez, J. Palacios-Alquisira, and J.M. Dominguez, On the limits of gas separation in CO_2/CH_4, N_2/CH_4 and CO_2/N_2 binary mixtures using polyimide membranes,, J Membr Sci, 293, 2007, 53.

[42] P. D. C. Dietzel, R. Blom, and H. Fjellvåg, Base-Induced Formation of Two Magnesium Metal-Organic Framework Compounds with a Bifunctional Tetratopic Ligand, Eur. J. Inorg. Chem. , 2008,
[43] S. Pu, J. Wang, L. Li, Z. Zhang, Z. Bao, Q. Yang, Y. Yang, H. Xing, and Q. Ren, Performance Comparison of Metal–Organic Framework Extrudates and Commercial Zeolite for Ethylene/Ethane Separation, Industrial & Engineering Chemistry Research, 57, 2018, 1645.
[44] S.A. FitzGerald, B. Burkholder, M. Friedman, J.B. Hopkins, C.J. Pierce, J.M. Schloss, B. Thompson, and J.L.C. Rowsell, Metal-Specific Interactions of H2 Adsorbed within Isostructural Metal–Organic Frameworks, Journal of the American Chemical Society, 133, 2011, 20310.
[45] X. Zheng, Y. Huang, J. Duan, C. Wang, L. Wen, J. Zhao, and D. Li, A microporous Zn(ii)–MOF with open metal sites: structure and selective adsorption properties, Dalton Transactions, 43, 2014, 8311.
[46] Z. Bao, L. Yu, Q. Ren, X. Lu, and S. Deng, Adsorption of CO2 and CH4 on a magnesium-based metal organic framework, Journal of Colloid and Interface Science, 353, 2011, 549.
[47] E.A. Feijani, A. Tavasoli, and H. Mahdavi, Improving Gas Separation Performance of Poly (vinylidene fluoride) Based Mixed Matrix Membranes Containing Metal − Organic Frameworks by Chemical Modification, Ind Eng Chem Res, 2015, 2015, 12124.
[48] J. F. Li, Z. L. Xu, H. Yang, L. Y. Yu, and M. Liu, Effect of TiO_2 nanoparticles on the surface morphology and performance of microporous PES membrane, Appl Surf Sci, 255, 2009, 4725.
[49] D.Q. Vu, W.J. Koros, and S.J. Miller, Mixed matrix membranes using carbon molecular sieves. I. Preparation and experimental results, J Membr Sci 211, 2003, 311.
[50] D. Yang, H.-Y. Cho, J. Kim, S.-T. Yanga, and W.-S. Ahn, CO2 capture and conversion using Mg-MOF-74 prepared by a sonochemical method, Energy Environ Sci, 5, 2012, 6465.
[51] S. Shahid and K. Nijmeijer, Performance and plasticization behavior of polymer–MOF membranes for gas separation at elevated pressures, J Membr. Sci., 470, 2014, 166.
[52] Z. Bao, L. Yu, Q. Ren, X. Lu, and S. Deng, Adsorption of CO_2 and CH_4 on a magnesium-based metal organic framework, J Colloid Interface Sci, 353, 2011, 549.
[53] A.O. Yazaydın, A. Benin, S.A. Faheem, P. Jakubczak, J.J. Low, R.R. Willis, and R.Q. Snurr, Enhanced CO_2 adsorption in metal-organic frameworks via occupation of open-metal sites by coordinated water molecules, Chem Mater, 21, 2009, 1425.
[54] M. Farnam, H. Mukhtar, and A.Z. Shariff, An investigation of blended polymeric membranes and their gas separation performance, RSC Advances, 6, 2016, 102671.
[55] W.J. Koros and G.K. Fleming, Membrane-based gas separation, Journal of Membrane Science, 83, 1993, 1.
[56] Y. Wang, X. Ma, B.S. Ghanem, F. Alghunaimi, I. Pinnau, and Y. Han, Polymers of intrinsic microporosity for energy-intensive membrane-based gas separations, Materials Today Nano, 3, 2018, 69.
[57] B. Comesaña-Gándara, J. Chen, C.G. Bezzu, M. Carta, I. Rose, M.-C. Ferrari, E. Esposito, A. Fuoco, J.C. Jansen, and N.B. McKeown, Redefining the Robeson upper bounds for CO2/CH4 and CO2/N2 separations using a series of ultrapermeable benzotriptycene-based polymers of intrinsic microporosity, Energy & Environmental Science, 12, 2019, 2733.
[58] T. Rodenas, I. Luz, G. Prieto, B. Seoane, H. Miro, A. Corma, F. Kapteijn, F. Llabrés i Xamena, and J. Gascon, Metal–organic framework nanosheets in polymer composite materials for gas separation, Nature Mater, 14, 2015, 48.
[59] A. Jomekian, R.M. Behbahani, T. Mohammadi, and A. Kargari, CO_2/CH_4 separation by high performance co-casted ZIF-8/Pebax 1657/PES mixed matrix membrane, J Natural Gas Sci Eng, 31, 2016, 562.
[60] A. Kilic, C. Atalay-Oral, A. Sirkecioglu, S.B. Tantekin-Ersolmaz, and M.G. Ahunbay, Sod-ZMOF/Matrimid (R) mixed matrix membranes for CO2 separation, Journal of Membrane Science, 489, 2015, 81.

Supporting Information for:

Mg–MOF–74/Polyvinyl acetate (PVAc) mixed matrix membranes for CO_2 separation

Srabani Majumdar[1], Begum Tokay[1,*], Violeta Martin-Gil[2], James Campbell[1], Roberto Castro-Muñoz[2], Mohd Zamidi Ahmad[2], Vlastimil Fila[2]

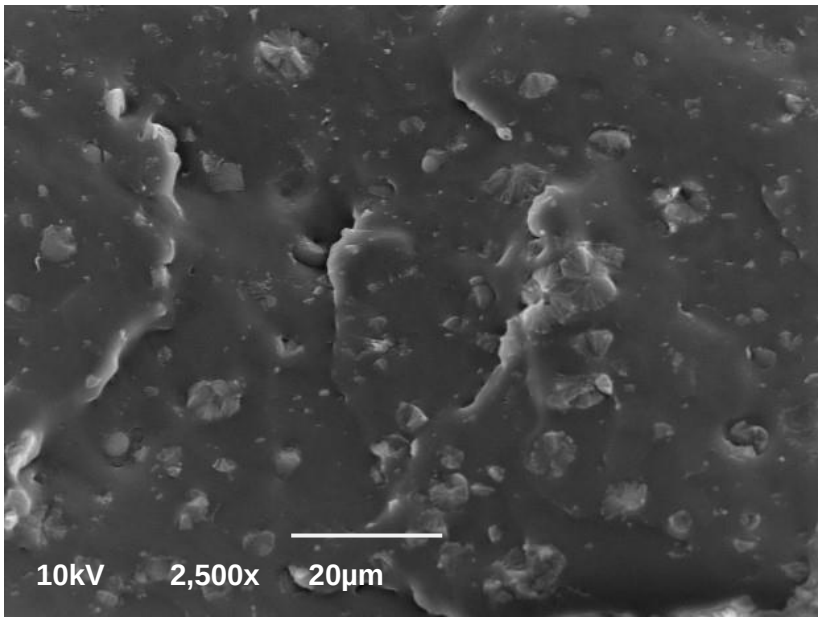

Fig. S1. SEM cross section image of MMM containing 20 wt% Mg-MOF-74.

Table S1. Mixed gas permeation properties of pure PVAc membranes and the MMMs loaded with 20 wt% of Mg-MOF-74 particles at 25 and 35 ºC.

Mg-MOF-74 wt% in PVAc	Separation temperature (ºC)	CO_2 permeability (Barrer)	CH_4 permeability (Barrer)	CO_2/CH_4 selectivity
0	25	0.71 ± 0.1	0.07 ± 0.03	10.6 ± 0.03
	35	1.3 ± 0.4	0.22 ± 0.1	6 ± 0.6
20	25	4.7 ± 0.1	0.2 ± 0.04	24.8 ± 0.2
	35	5.1 ± 1.4	0.7 ± 0.1	7.5 ± 0.4